PARTIALLY ADAPTIVE BROADBAND BEAMFORMING WITH A SUBBAND-SELECTIVE TRANSFORMATION MATRIX

Wei Liu, Stephan Weiss, and Lajos Hanzo

Communications Research Group
Dept. of Electronics & Computer Science
University of Southampton, SO17 1BJ, U.K.
{w.liu, s.weiss, l.hanzo}@ecs.soton.ac.uk

ABSTRACT

In this paper, a partially adaptive generalized sidelobe canceller (GSC) with a novel spatially/spectrally subband-selective transformation matrix is proposed. The row vectors of this matrix constitute a series of bandpass filters, which separate the blocking matrix outputs into components of different DOAs and frequencies. This results in bandlimited spectra of its outputs, which is further exploited by subband decomposition and discarding the low-pass subbands appropriately prior to running independent unconstrained adaptive filters in subbands. By these steps the computational complexity of the system is greatly reduced. Additionally, a faster convergence speed is achieved by joint spatial and spectral decorrelation.

1. INTRODUCTION

Adaptive beamforming has found many applications in various areas ranging from sonar and radar to wireless communications [1]. A beamformer with M sensors receiving a signal of interest from the direction of arrival (DOA) θ is shown in Fig. 1. To perform beamforming with high interference rejection and resolution, arrays with a large number of sensors and filter coefficients have to be employed and the computational burden of a fully adaptive processor thus becomes considerable. A popular way to reduce the computational complexity are partially adaptive beamformers, which employ only a subset of available degrees of freedom (DOF) in the filter weight update process at the expense of a somewhat reduced performance [2].

Partially adaptive techniques have been studied widely and many ideas have been proposed such as the weight reduction transformation [3] and the eigencanceller [4]. In this paper, with a GSC [5] as the underlying structure, a novel spatially/spectrally subband-selective transformation matrix following the blocking matrix is proposed for partially adaptive broadband beamforming. The row vectors of this matrix constitute a series of bandpass filters, which separate the interfering signals into components of different DOAs and frequencies. This results in bandlimited spectra of its outputs, and is further exploited by subband decomposition and discarding the low-pass subbands appropriately prior to running independent unconstrained adaptive filters in each non-redundant subband. Moreover, the design and implementation of this transformation matrix are simplified by a cosine-modulated version. By these steps the computational complexity of the system is greatly reduced and a faster convergence speed is also achieved by joint spatial and spectral decorrelation.

The paper is organised as follows. Sec. 2 briefly reviews GSC based partially adaptive broadband beamforming. We propose a spatially/spectrally subband-selective transformation matrix in Sec. 3, whereas the design of such a matrix is described in Sec. 4. Finally, simulation results are given in Sec. 5 and conclusions drawn in Sec. 6

2. PARTIALLY ADAPTIVE GENERALISED SIDELOBE CANCELLER

A linearly constrained minimum variance (LCMV) beamformer [6] performs the minimisation of the variance or

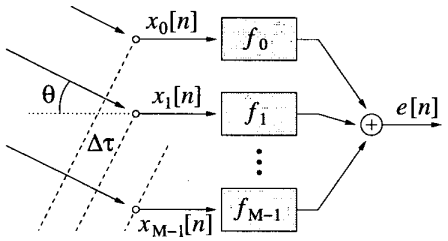

Fig. 1: A beamformer with linear array.

0-7803-7551-3/02/$17.00 ©2002 IEEE

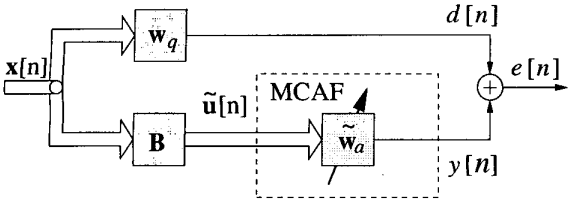

Fig. 2: A generalized sidelobe canceller, where adaptive optimisation is performed by a multichannel adaptive filter (MCAF).

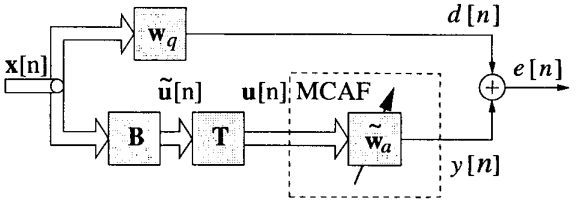

Fig. 3: A partially adaptive GSC by a transformation matrix.

power of the output signal with respect to some given spatial and spectral constraints. For a beamformer with M sensors and a J-tap filter following each sensor, the output $e[n]$ can be expressed as

$$e[n] = \mathbf{w}^H \mathbf{x}, \tag{1}$$

where coefficients and input sample values are defined as

$$\mathbf{w} = [\mathbf{w}_0^T \ \mathbf{w}_1^T \ \dots \ \mathbf{w}_{J-1}^T]^T, \tag{2}$$

$$\mathbf{w}_j = [w_{0,j} \ w_{1,j} \ \dots \ w_{M-1,j}]^H, \tag{3}$$

$$\mathbf{x} = [\mathbf{x}^T[n] \ \mathbf{x}^T[n-1] \ \dots \ \mathbf{x}^T[n-J+1]]^T, \tag{4}$$

$$\mathbf{x}[n-j] = [x_0[n-j] \ x_1[n-j] \ \dots \ x_{M-1}[n-j]]^T \tag{5}$$

where $\{\cdot\}^T$ and $\{\cdot\}^H$ are transpose and Hermitian transpose, respectively. Each vector $\mathbf{w}_j$, $j = 0(1)J-1$, contains the M complex conjugate coefficients sitting at the jth tap position of the filters f_m, $m = 0(1)M-1$ and $\mathbf{x}[n-j]$, $j = 0(1)J-1$, holds the jth data slice corresponding to the jth coefficient vector $\mathbf{w}_j$.

The LCMV problem can be formulated as

$$\min_{\mathbf{w}} \mathbf{w}^H \mathbf{R}_{xx} \mathbf{w} \qquad \text{subject to} \qquad \mathbf{C}^H \mathbf{w} = \mathbf{f} \ , \tag{6}$$

where $\mathbf{R}_{xx}$ is the covariance matrix of observed array data in $\mathbf{x}$, $\mathbf{C} \in \mathbb{C}^{MJ \times SJ}$ is a constraint matrix and $\mathbf{f} \in \mathbb{C}^{SJ}$ is the $SJ \times 1$ response vector. The constraint matrix imposes derivative constraints of order $S-1$ [7].

The constrained optimisation of the LCMV problem in (6) can be conveniently solved using a GSC as shown in Fig. 2. The GSC performs a projection of the data onto an unconstrained subspace by means of a blocking matrix $\mathbf{B}$ and a quiescent vector $\mathbf{w}_q$. Thereafter, standard unconstrained optimisation algorithms such as least mean square (LMS) or recursive least squares (RLS) algorithms can be invoked [8]. Fig. 2 shows the principle of a GSC, where a desired signal $d[n]$ is obtained via $\mathbf{w}_q$,

$$d[n] = \mathbf{w}_q^H \cdot \mathbf{x}_n \qquad \text{with} \quad \mathbf{w}_q = \mathbf{C}(\mathbf{C}^H\mathbf{C})^{-1}\mathbf{f} \ . \tag{7}$$

For derivative constraints of order $S-1$, the blocking matrix can be formed in the following [9]

$$\mathbf{B} = \mathbf{B}_M \cdot \mathbf{B}_{M-1} \cdots \mathbf{B}_{M-S+1}, \tag{8}$$

where

$$\mathbf{B}_i = \begin{bmatrix} 1 & -1 & & & \mathbf{0} \\ & \ddots & \ddots & & \\ & & \ddots & \ddots & \\ & & & \ddots & \ddots \\ \mathbf{0} & & & 1 & -1 \end{bmatrix}^T \in \mathbb{C}^{i \times i-1} \tag{9}$$

with $i = M, M-1, \cdots, M-S+1$.

The blocking matrix output $\tilde{\mathbf{u}}[n] \in \mathbb{C}^{M-S \times 1}$ is obtained by $\tilde{\mathbf{u}}[n] = \mathbf{B}^H \mathbf{x}[n]$. For a partially adaptive GSC, the dimension of $\tilde{\mathbf{u}}[n]$ is further reduced by a transformation matrix $\mathbf{T} \in \mathbb{C}^{L \times M-S}$ [3], which is shown in Fig. 3. The multi-channel input $\mathbf{u}[n] \in \mathbb{C}^{L \times 1}$ to the following adaptive process is obtained by $\mathbf{u}[n] = \mathbf{T}\tilde{\mathbf{u}}[n]$, where

$$\mathbf{T} = [\mathbf{t}_0 \ \mathbf{t}_1 \ \dots \ \mathbf{t}_{L-1}]^T, \tag{10}$$

$$\mathbf{t}_l = [t_l[0] \ t_l[1] \ \dots \ t_l[M-S-1]] \tag{11}$$

with $l = 0(1)L-1$.

For partial adaptivity, $L < M-1$, which results in a reduced number of DOFs and offers reduced complexity traded off against a somewhat inferior performance. In the next section, we will trade the loss of DOFs against a specific design of the transformation matrix.

3. SPATIALLY/SPECTRALLY SELECTIVE TRANSFORMATION

Consider an impinging signal $e^{-j\omega t}$ with DOA angle θ. Referring to Fig. 1, the waveform impinges with a time delay $\Delta\tau$ on adjacent sensors separated by d in a medium with propagation speed c. The received phase vector at the sensor array, $\underline{X}$, is

$$\underline{X} = \left[1 \ e^{-j\omega\Delta\tau} \dots e^{-j\omega(M-1)\Delta\tau}\right]^T \text{ with } \Delta\tau = \frac{d}{c}\sin\theta. \tag{12}$$

Assume that the array sensors are spaced by half wavelength of the maximum signal frequency and the temporal sampling frequency ω_s is two times the maximum signal frequency, i.e. $d = \lambda_s = cT_s$, where T_s is the temporal sampling period. Then, we get $\Delta\tau = T_s \sin\theta$. Noting $\omega T_s = \Omega$, where Ω is the normalised angular frequency of the signal, the phase vector becomes

$$\underline{X} = \left[1 \quad e^{-j\Omega \sin\theta} \quad \cdots \quad e^{-j(M-1)\Omega \sin\theta}\right]^T . \qquad (13)$$

Using the substitution $\Psi = \Omega \sin\theta$ and equation (8), the output of the blocking matrix can be expressed as

$$\tilde{\mathbf{u}}[n] = (1 - e^{-j\Psi})^S \cdot \left[1 \quad e^{-j\Psi} \quad \cdots \quad e^{-j(M-2)\Psi}\right]^T \cdot e^{jn\Omega} . \qquad (14)$$

Then the $l-$th output of the transformation matrix, $u_l[n]$, $l = 0(1)L-1$, can be denoted as

$$\begin{aligned} u_l[n] &= \mathbf{t}_l \cdot \tilde{\mathbf{u}}[n] \\ &= (1 - e^{-j\Psi})^S \sum_{m=0}^{M-2} t_l[m] e^{-jm\Psi} e^{jn\Omega} \\ &= (1 - e^{-j\Psi})^S \cdot T_l(e^{j\Psi}) \cdot e^{jn\Omega}, \qquad (15) \end{aligned}$$

with $T_l(e^{j\Psi}) \bullet\!\!-\!\!\circ\, t_l[m]$ being a Fourier transform pair. When $\theta = 0$, this output will be zero, i.e. the signal of interest from broadside is blocked. Now we study the effect of $T_l(e^{j\Psi})$ and arrange $T_l(e^{j\Psi})$, $l = 0(1)L-1$, on the interval $\Psi \in [0; \pi]$ as shown in Fig. 4, such that

$$T_l(e^{j\Psi}) = \begin{cases} 1 & \text{for } \Psi \in [\Psi_{l,\text{lower}}; \Psi_{l,\text{upper}}] \\ 0 & \text{otherwise} \end{cases} . \qquad (16)$$

As $\sin\theta \in [0; 1]$ when $\theta \in [0; \frac{\pi}{2}]$, the possible maximum frequency component of the lth output $u_l[n]$ is $\Omega = \pi$ while the possible minimum frequency component is $\Omega = \Psi_{l,\text{lower}}$. Therefore we have

$$T_l(e^{j\Omega \sin\theta}) = \begin{cases} 1 & \text{for } \Omega \in [\Psi_{l,\text{lower}}; \pi] \\ 0 & \text{otherwise} \end{cases} . \qquad (17)$$

By this arrangement, the transformation matrix decomposes its input signals in both the spatial and temporal domains and its row vectors perform a temporal high-pass filtering operation according to the DOA angle. With increasing l, these filters are associated with a tighter and tighter highpass spectrum and the last output $(L-1)$ only contains the ultimate highpass component. Thus, if we decompose each of these highpass signals into subbands in a similar way as in [10], the subband signals in the corresponding lowpass subbands will be zero and can be omitted from subsequent processing. The subband setup is shown in Fig. 6.

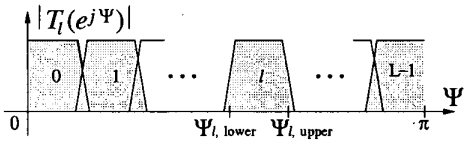

Fig. 4: Arrangement of the L column vectors in $\mathbf{T}$.

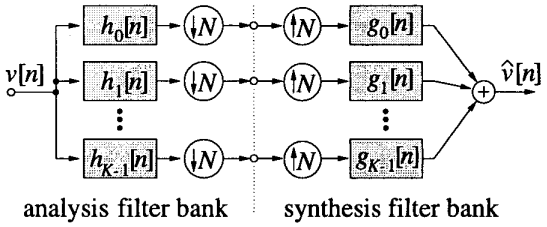

Fig. 5: K-channel filter banks with decimation ratio N.

The blocks labelled A perform analysis operations, splitting the signal into K frequency bands by a $K-$channel filter bank with decimation ratio N, which is shown in Fig. 5. Within each subband, an independent unconstrained multichannel adaptive filter (MCAF) is operated, and a synthesis filter bank, labelled S, recombines the different subsystem outputs to a fullband beamformer output $e[n]$.

Now we analysis the computational complexity of this system. For the subband decomposition and adaptation itself, a reduction of approximately K/N^2 (K/N^3) of the operations required for a fullband adaptive algorithm with a complexity of $\mathcal{O}(L_a)$ ($\mathcal{O}(L_a^2)$) is achieved, where L_a is the total number of coefficients in the fullband realisation [10]. If sufficiently selective column vectors $\mathbf{t}_l$ can be designed, the first ($k = 0$) MCAF would be a single channel adaptive filter drawing its low frequency input solely from the first branch of $\mathbf{B}$. The second ($k = 1$) MCAF block in Fig. 6 will most likely only cover some of the lower branches of $\mathbf{T}$, while finally only the last MCAF ($K-1$) consists of L

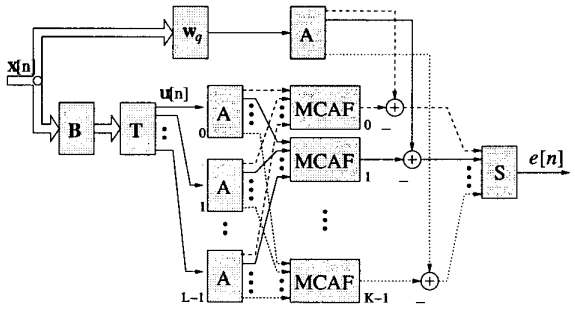

Fig. 6: A Subband-selective GSC, where an independent MCAF is applied to each subband.

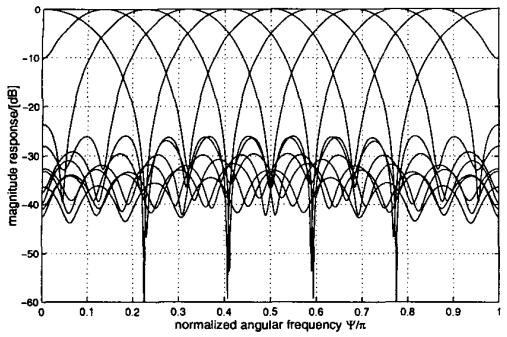

Fig. 7: A design example for a 10×16 transformation matrix.

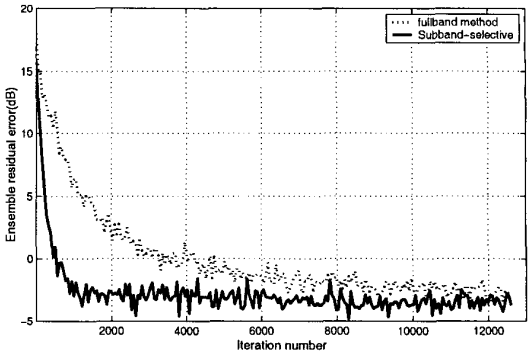

Fig. 8: Learning curves for simulation I (stepsize=0.25).

non-sparse channels. Thus, under ideal conditions, the dimensionality of the MCAFs can be reduced by half, with a proportional decrease in computational complexity. Considering the overall subband-selective GSC system, it requires approximately $\frac{LK}{2(M-S)N^2}$ or $\frac{LK}{2(M-S)N^3}$ of computations of the traditional fully adaptive GSC schemes.

4. DESIGN OF THE TRANSFORMATION MATRIX

In the above subband-selective GSC, the transformation matrix plays a central role and the row vector design with a good band-selective property is of great importance. We may design each of these vectors separately. However, to reduce the design and implementation complexity of the transformation matrix, we propose a cosine-modulated version.

Assume the prototype vector is $h[m], m = 0(1)M\text{–}S\text{–}1$, then $t_l[m], l = 0(1)L-1$, can be obtained by [11]

$$t_l[m] = h[m]\cos\left[\frac{\pi}{2L}(2l+1)(m-\frac{M-S-1}{2})+(-1)^l\frac{\pi}{4}\right]. \tag{18}$$

Thus, the design problem of the transformation matrix is simplified to the design of a low-pass prototype filter $h[m]$, which can be easily solved by some common filter design algorithms, such as the *remez* function in MATLAB. Here we give a result obtained by the subroutine BCONF in the IMSL library [12] for a 10×16 transformation matrix, which is shown in Fig. 7.

5. SIMULATIONS AND RESULTS

The simulations are based on a beamformer setup with $M = 17$ sensors and $J = 70$ taps for each fullband MCAF channel. The signal of interest comes from broadside and with a signal to interference ratio (SIR) of -24 dB and signal to noise ratio (SNR) of 20 dB. The filter banks we employ are 12-channel oversampled generalised DFT filter banks [13] with decimation factor $N = 10$. The length of the adaptive filter in each subband MCAF channel is $J/N = 7$. We use a normalised LMS algorithm for adaptation.

For a first simulation (simulation I), the interfering signal comes from the DOA angle of 20° and covers the frequency interval $\Omega = [0.15\pi; 0.85\pi]$. For a second scenario (simulation II), we have two interfering signals covering the frequency interval $[0.15\pi; 0.45\pi]$ and $[0.55\pi; 0.85\pi]$, with DOA angles of 20° and 40°, respectively.

Simulation results are shown in Fig. 8 and 9, while Fig. 10 shows the steady-state directivity pattern of simulation II. From the result, we can see that, with its lower computational complexity, the subband-selective system outperforms the fullband counterpart in terms of convergence speed because of its combined spatial and spectral decorrelation effect.

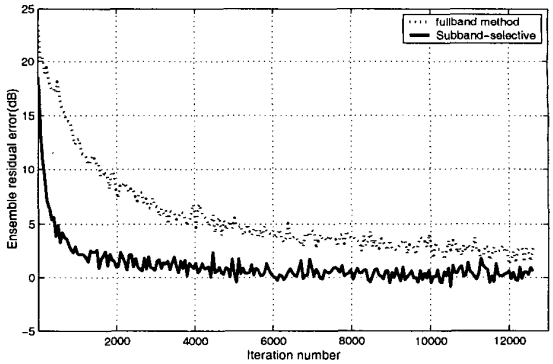

Fig. 9: Learning curves for simulation II (stepsize=0.45).

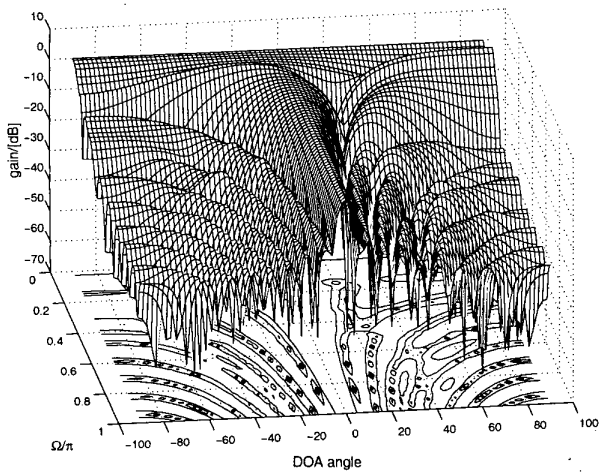

Fig. 10: Steady-state directivity pattern of simulation II.

6. CONCLUSIONS

A subband-selective GSC for partially adaptive broadband beamforming with a subband-selective transformation matrix has been proposed, where its row vectors constitute a series of bandpass filters, which decompose the input signals into components of specific DOA angles and frequencies and lead to band-limited spectra of its outputs. Subband methods are employed to remove their redundancy by discarding the corresponding lowpass subbands. The combination of partial adaptation, subband decomposition and discarding permit a considerably reduced computational complexity. As demonstrated in simulations, our approach also has the additional benefit of faster convergence for LMS-type adaptive algorithms.

7. REFERENCES

[1] L. C. Godara, "Application of Antenna Arrays to Mobile Communications, Part I: Performance Improvement, Feasibility, and System Considerations," *Proceedings of the IEEE*, vol. 85, no. 7, pp. 1031–1060, July 1997.

[2] D. J. Chapman, "Partial Adaptivity for Large Arrays," *IEEE Transactions on Antennas and Propagation*, vol. 24, no. 9, pp. 685–696, September 1976.

[3] B. D. Van Veen and R. A. Roberts, "Partially Adaptive Beamforming Design via Output Power Minimization," *IEEE Transactions on Acoustics, Speech, and Signal Processing*, vol. 35, pp. 1524–1532, 1987.

[4] B. D. Van Veen, "Eigenstructure Based Partially Adaptive Array Design," *IEEE Transactions on Antennas and Propagation*, vol. 36, no. 1, pp. 357–362, January 1988.

[5] L. J. Griffith and C. W. Jim, "An Alternative Approach to Linearly Constrained Adaptive Beamforming," *IEEE Transactions on Antennas and Propagation*, vol. 30, no. 1, pp. 27–34, January 1982.

[6] O. L. Frost, III, "An Algorithm for Linearly Constrained Adaptive Array Processing," *Proceedings of the IEEE*, vol. 60, no. 8, pp. 926–935, August 1972.

[7] K. M. Buckley and L. J. Griffith, "An Adaptive Generalized Sidelobe Canceller with Derivative Constraints," *IEEE Transactions on Antennas and Propagation*, vol. 34, no. 3, pp. 311–319, March 1986.

[8] S. Haykin, *Adaptive Filter Theory*, Prentice Hall, Englewood Cliffs, 2nd edition, 1991.

[9] N. K. Jablon, "Steady State Analysis of the Generalized Sidelobe Canceler by Adaptive Noise Canceling Techniques," *IEEE Transactions on Antennas and Propagation*, vol. 34, no. 3, pp. 330–337, March 1986.

[10] W. Liu, S. Weiss, and L. Hanzo, "Subband Adaptive Generalized Sidelobe Canceller for Broadband Beamforming," in *Proc. IEEE Workshop on Statistical Signal Processing*, Singapore, August 2001, pp. 591–594.

[11] R. D. Koilpillai and P. P. Vaidyanathan, "Cosine-modulated FIR Filter Banks Satisfying Perfect Reconstruction," *IEEE Transactions on Signal Processing*, vol. 40, pp. 770–783, April 1992.

[12] Visual Numerics Inc., *IMSL Fortran Numerical Libraries*.

[13] S. Weiss and R. W. Stewart, *On Adaptive Filtering in Oversampled Subbands*, Shaker Verlag, Aachen, Germany, 1998.